

RECEIVED
CENTRAL FAX CENTER

OCT 13 2005

**CERTIFICATE OF
FACSIMILE
TRANSMISSION
TRANSMISSION OF
REFERENCES**

Application Number	10/694,548
Filing Date	10/27/2003
First Inventor	MacDonald, Stuart G.
Examiner Name	Bockelman, Mark
Art Unit	3762
Docket Number	SGM-521

Faxed to Number 1-571-273-8300Total Pages 10

DATE OF TRANSMISSION: 10/13/2005

TITLE OF CASE:

Biothermal Power Source and Method for Implantable Devices

The following documents are enclosed:

Certificate of Facsimile Transmission (1 page)

Letter (1 page)

References (8 pages)

The above named documents are being facsimile transmitted to the United States Patent and Trademark Office on the date indicated above. The Director is authorized to charge any additional fee(s) as needed during the pendency of this application to deposit account 50-2753.

Howard J. Greenwald P.C.
349 W. Commercial Street, Suite 2490
East Rochester, NY 14445
Telephone (585) 387-0285
Fax (585) 387-0288

Signature of Transmitter: Peter J. Mikesell

Howard J. Greenwald, Reg. No. 24,247
 Peter J. Mikesell, Reg. No. 54,311
 William J. Six

PLEASE NOTE: This facsimile message may contain information which is privileged, confidential, and exempt from disclosure under applicable laws and is intended only for the use of the individual named above and others who have been specifically authorized to receive it. If you are not the intended recipient, you are hereby notified that any dissemination, distribution or copying of the communication is strictly prohibited. If you have received this communication in error, please notify the law offices of HOWARD J. GREENWALD P.C. immediately by telephone at (585) 387-0285. You will be reimbursed for your telephone expense.

FIRST AVAIL. COPY

RECEIVED
CENTRAL FAX CENTER

OCT 13 2005

Application No.	10/694,548
Applicant	MacDonald, Stuart G.
Filed	10/27/2003
Title	Biothermal Power Source and Method for Implantable Devices
TC/A.U.	3762
Examiner	Bockelman, Mark
Docket No.	SGM-521

Honorable Commissioner for Patents
P.O. Box 1450
5 Alexandria, VA 22313-1450

ADDENDUM TO AMENDMENT

Sir:

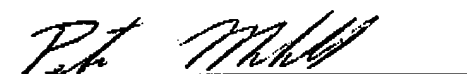
- The 10/7/05 amendment referred to several non-patent references.
 10 Enclosed herewith, for the Examiner's convenience, please find copies of these references.

CERTIFICATE OF MAILING OR TRANSMISSION

- I hereby certify that this paper is being deposited with the United States Postal Service with sufficient postage for first class mail in an envelope addressed to the Commissioner for Patents, PO Box 1450, Alexandria, Virginia 22313-1450, or being facsimile transmitted to the USPTO, on the date indicated below:

Date 10/13/2005

20



Peter J. Mikesell, Reg. No. 54,311

Nanomedicine, Volume I: Basic Capabilities

RECEIVED
CENTRAL FAX CENTER

OCT 13 2005

© 1999 Robert A. Freitas Jr. All Rights Reserved.

Robert A. Freitas Jr., Nanomedicine, Volume I: Basic Capabilities, Landes Bioscience, Georgetown, TX, 1999

Vol. 1 Index Contents Search Home Help About

8.4.1 Thermographic Navigation

8.4.1.1 Thermography of the Human Body

The human body presents a complex and temporally varying spatial temperature field. The external parts of the body have a lower mean temperature than the internal parts, with temperature decreasing along the longitudinal axis of the extremities, producing both axial and radial temperature gradients. The differing heat production of individual organs, geometric irregularities, changes in insulation and evaporation, convective heat transport via the blood, and the diurnal and other periodic variations³³²⁷ add further complexities to the thermal map.³⁹⁰

The homeothermic core of the body is distinguishable from the shell, which most readily responds to environmental fluctuations. The core generally consists of the interior of the thorax and abdomen, the brain, and part of the skeletal muscles. With moderate changes in ambient temperature, the shell normally comprises the outermost 20%-35% of the human body.^{894,895} However, during extreme chilling, the shell may enlarge to ~50% of total body volume, equivalent to a mean layer thickness of 2.5 cm.⁸⁹⁰ Figure 8.28 shows the overall distribution of tissue temperatures as a series of isotherms.

Skin temperatures display the greatest thermographic variability in response to external factors. For example, nude humans standing for 3 hours in a cold room (5°C, 50% relative humidity, 0.1-0.2 m/sec wind speed) experience skin temperature differentials up to 15°C (= 13°C to 28°C), with the lowest temperatures in fingers and toes, the highest in trunk and forehead, and average core/surface gradient ~1.5°C.⁸⁹⁶ Heat loss is ~10% lower for females due to their thicker layer of subcutaneous fat, making their cold-room skin temperature slightly lower than for males.³⁹⁸ After 3 hours in a hot room (50°C), skin temperature differentials amounted to only 2.5°C (= 35°C to 37.5°C), with an average core/surface gradient of ~1°C.⁸⁹⁴ With normal clothing in a room at 15-20°C, mean skin temperature is 32-35°C.

Skin thermography of the human head was first reported by Edwards and Burton;⁸⁹⁷ skin v.s. rectal temperatures at various ambient temperatures are well-studied.^{893,898} Skin temperature patterns in neonates reflect near uniform heat conduction through the tissues.²¹⁷ In childhood, specific patterns develop into a stable, permanent adult pattern.⁹¹⁶ The dermathermal patterns differ in lean and obese patients, and exhibit a continual state of small rhythmic change. These changes — probably a result of active vasodilation due to sympathetic innervation over most of the human skin area⁹¹⁹ — are observed over the arms, hands, trunk and head, but are not all in phase with each other, nor even of the same amplitude.^{918,919,3334-3338} Skin thermology, including infrared thermography, is now an important branch of medical diagnostic imaging.^{899,912} Subcutaneous (shell) temperatures generally increase with depth.

Human core (rectal) temperature averages 37.0°C,⁸²⁴ but this simple number hides considerable natural variation (Table 8.11). The temperatures of inner organs vary by 0.2-1.2°C under normal room conditions, and by up to 0.9°C within individual organs.⁸⁹⁰ Temperature gradients within the brain amount to 1.4°C; the cortex is cooler than the basal regions, with incoming blood cooler than the central brain tissue.⁹⁰⁰ Brain temperature also decreases during sleep and rises during periods of emotional arousal.⁹⁰¹ Cooling or warming the skin of the head causes temperature changes in the tympanic membrane (Fig. 7.3) of up to 0.4°C due to the returning venous blood.⁹⁰² Oral temperature can have wide variation, depending for example on the thermal character of recently ingested food and drink, <http://www.nanomedicine.com/NMI/8.4.1.1.htm>

9/20/2005

under cool room conditions. skin is at 35C, so

Quantum Well Thermoelectric Devices

S. Ghemaly and N. B. Elsner
Hi-Z Technology, Inc.
San Diego, California 92126
MRS December 2003

See p 3

Abstract

This paper discloses the recent developments of high efficiency quantum well thermoelectrics at Hi-Z Technology, Inc. The performance of the latest P type B_xC_yB_z-N type Si/SiGe couple will be presented as well as data for the new N-type Si/SiC that will replace Si/SiGe and improve couple efficiency.

Preliminary calculations regarding the development of actual quantum well modules will be presented for power prediction. These modules can be used in future energy conversion system as well as air conditioning system designs.

Our current efforts to produce quantum well films more rapidly will be discussed.

Introduction

Hi-Z Technology, Inc. (Hi-Z) is currently developing many different thermoelectric generator designs that are used to convert waste heat or heat sources directly to electricity. These include waste heat recovery from diesel trucks as well as automobiles and thermoelectric power generator including space application.

Bismuth telluride based materials are presently used for power generation in remote locations, for example in deep space probes or direct conversion in general. Usage in direct conversion is conditional upon improvement in the efficiency of energy conversion from heat into electricity. The efficiency of thermoelectric energy conversion devices is strongly limited by the performance of the materials, which is normally measured in terms of a *Figure of Merit Z* (see next section).

Increasing the figure of merit of thermoelectric materials is difficult and basic properties of the materials. The breakthrough approach to increasing Z is to form compositionally modulated materials, mainly by QW confinement of carriers in the active layers in a multilayer film by adjacent barrier layers. The core concept is to enclose each electrically active layer by a material which has a band offset sufficient to form a barrier for the charge carriers. The major improvement in Z is expected to follow from an increased Seebeck coefficient that results from an increase in the density of states. There may also be a significant effect on the carrier mobility due to quantum confinement, so ideally there would be improvement in Z from f the Seebeck coefficient, conductivity, and thermal conductivity. QW effects become significant only when the thickness of the active layer is small, below about 200 Å. The effectiveness of QW confinement and its effect on the figure of merit depends on many factors such as the carrier concentration, which is temperature dependent.

In addition to QW confinement, improvement in Z may result from the periodicity of the multiple film structure on the thermal conductivity [1]. At low values of the thickness of individual layers, there may be interference with the propagation of phonon modes, and therefore a reduction in κ_z . The theory of this effect, and its application to both in-plane and through-plane thermal conductivity values, is now a subject of intense research and may

evolve into a field of engineered thermal transport semi-independently of thermoelectricity [28-31].

Recent Advances

Hu-Z currently use conventional Bi_2Te_3 alloys thermoelectric modules. The material in these modules has a value of ZT [figure of merit (Z) times its mean absolute operation temperature (T)] of about 1. As shown in Figure 1, the value of ZT has hovered around 1 since the mid-1950s when semi-conductor materials were introduced into thermoelectric conversion. In the late 1990s new materials, including quantum well materials, started to increase the value of ZT to a cut 4 with some promise that even higher values can be obtained as development continues.

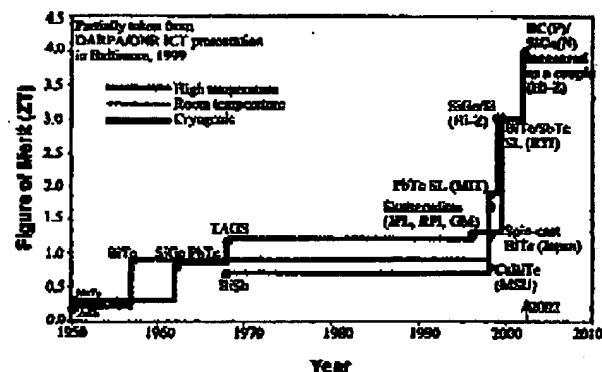


Figure 1: ZT Time Line

The figure of merit (Z) for a thermoelectric material is obtained from its electric and thermal properties by

$$Z = \sigma^2 / \rho^* x$$

where α is the Seebeck coefficient of the material, v/K , ρ is its resistivity, ohm-cm, and κ is its thermal conductivity, W/cm K. Efforts to improve the value of Z for a bulk material often fails because as one increases α , the values of ρ and/or κ usually also increase so that the resulting value of Z either remains the same or decreases. In 1992 Hicks and Duselhouse [1] of MIT suggested that quantum wells should be a good candidate for thermoelectric energy conversion. This was confirmed in 1998 when Ghemaly and Elsner of Hi-Z [5] measured the thermoelectric properties of Si/SiGe quantum well films produced by both UCLA and the Navy for purposes other than thermoelectric energy conversion. Since then several investigators around the country have confirmed the improved thermoelectric properties of quantum well films.

Quantum well films have been made by several methods. The Navy films measured by Hi-Z were made by molecular beam epitaxy (MBE). Currently Hi-Z is making its films by magnetron sputtering. Several other methods of film fabrication are possible. While magnetron sputtering does not result in quantum well films with thermoelectric properties quite as good as films made by MBE, they can be made much more quickly and therefore have the potential for much lower cost.

- Si/SiGe: Multilayer Quantum Well film thermoelectrics
- P-type B₄C/B₂C: High temperature thermally stable multilayer Quantum Well films
- Si/SiC Quantum Well development underway to replace Si/SiGe for power (higher temperature) applications

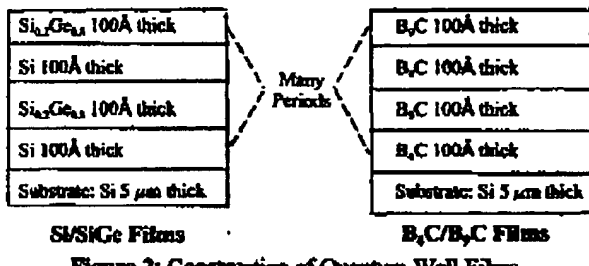


Figure 2: Construction of Quantum Well Films

A quantum well film is formed by alternating thin (~100 Å) layers of two materials with differing electron band gaps such as Si and SiGe as shown in Figure 2. When done correctly, all three of the thermoelectric properties improve, i.e., α increases and ρ and K decrease. This results in a much improved ZT and therefore an improved conversion efficiency (η) because η , which is defined by the equation:

$$\eta = \frac{T_H - T_C}{T_H} \times \frac{M-1}{M + \frac{T_C}{T_H}}$$

where the matching factor, M, is given by:

$$M = \sqrt{1 + \frac{Z}{2} (T_C + T_H)}$$

where T_C and T_H are respectively the cold and hot junction absolute temperatures. One will note that the first term of the efficiency equation is the Carnot efficiency.

Figure 3 is a graph of conversion efficiency as a function of ZT for various values of T_H and a value of T_C equal to 50°C. One can see that for even modest values of T_H , such as 250°C, and a value of $ZT = 4$, one can exceed a conversion efficiency of 20%.

A quantum well film useful in a thermoelectric module is made by making many periods of alternating 100 Å layers. These layers are typically formed on a substrate such as silicon, which can remain as part of the film. If the substrate does remain, it becomes a parasitic loss in the system. This problem is discussed

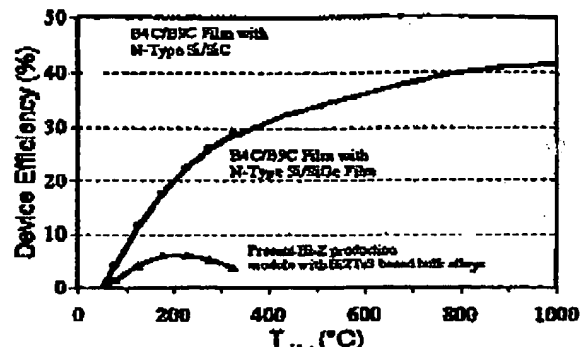


Figure 3: Calculated Couple Efficiency Versus Hot Side Temperature for B₄C/B₂C P-leg With a Si/SiGe or Si/SiC N-leg later.

The first quantum well couple was reported in 2002 [6] and yielded 14% efficiency. Unfortunately it was accidentally destroyed by overheating.

A second quantum well couple was completed recently. This couple shown in Figure 4 consists of B₄C/B₂C for the P leg and Si/SiGe for the N leg. Both films were a total of 11 μm thick and were deposited on a 5 μm thick Si substrate. Figure 5 is a graph of the uncorrected module conversion efficiency as a function of the hot junction temperature and shows a conversion efficiency of over 14% at a T_H of 250°C. No corrections were made for heat loss through the leads, by radiation, or through the substrate.

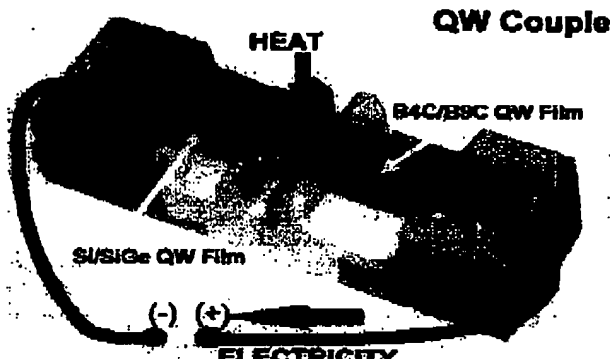


Figure 4: Experimental Quantum Well Couple

Table 1 presents the raw data taken at a T_H of 250°C and T_C of 70°C both for the quantum well couple and a calibration couple made of bulk bismuth-telluride alloy couple taken on the same test rig.

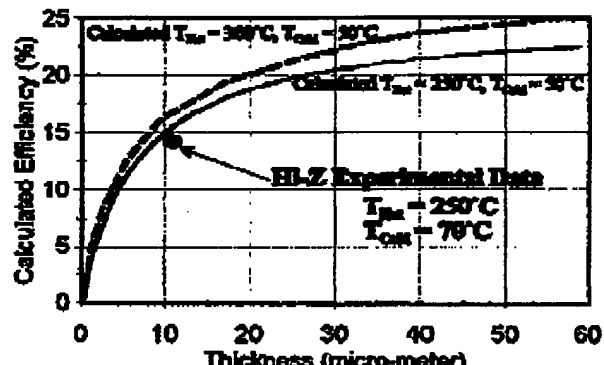
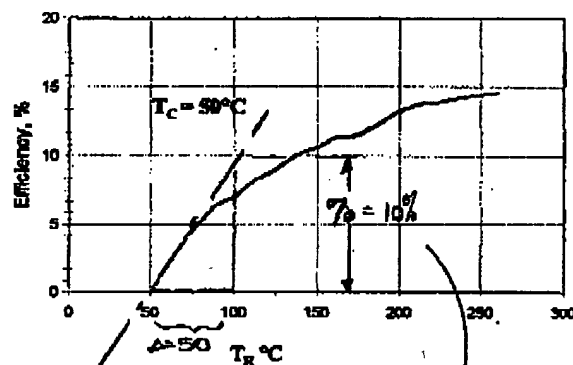
As previously mentioned, the substrate used will cause parasitic losses. Figure 6 presents a graph of the calculated quantum well conversion efficiency as a function of film thickness for films deposited on a 5 μm Si substrate for a T_H of 250°C and a T_C of 50°C. One can see that the curve appears to become asymptotic to about 25% efficiency for infinitely thick films. Also shown on the graph are the data from the test couple and that we plan to achieve of over 20% conversion efficiency at a film thickness of ~40 μm.

Table 1. QW Device Raw Test Data for 11 μm Thick $\text{B}_4\text{C}/\text{B}_2\text{C}$ and Si/SiGe on 5 μm Si at $T_{\text{hot}} = 70^\circ\text{C}$ and $T_{\text{cold}} = 250^\circ\text{C}$

	Power Into Heater			Power Out From Couple			Efficiency
	Voltage	Current	Power	Voltage	Current	Power	
$\text{B}_4\text{C}/\text{B}_2\text{C}-\text{Si}/\text{SiGe}$	0.1413V	47.1 mA	6.657 mW	0.365 V	2.608 mA	0.952 mW	14.30%
Calibration: Bi_2Te_3 Alloys	2.510	0.836 A	2.098 W	0.034 V	3.15 A	0.107 W	5.10%

Table 2. Thermoelectric Properties of Recently Fabricated Multi-layered QW Si/SiC Sputtered Film. Power number (α^2/ρ) of QW Si/SiC is ~250 compare to bulk Bi_2Te_3 power number of ~35.

Samples at Room Temperature	Thickness (Å)	ρ , Resistivity (mΩ·cm)	α , Seebeck Coefficient (μV/°C)
03-01	400	2.15	-750
03-02	800	2.16	-755
03-03	1000	2.14	-745
03-04	1000	2.12	-753
03-05	1600	2.15	-754
03-06	1600	2.11	-758
03-07	1400	2.17	-760
03-08	1400	2.14	-750
03-09	1600	2.12	-752
03-10	1600	2.14	-755



Hi-Z has also been depositing quantum well films of Si/SiC. This is a N-type quantum well and can be used with the $\text{B}_4\text{C}/\text{B}_2\text{C}$ P-type film for higher temperature applications. Table 2 presents the thermoelectric properties data obtained for several Si/SiC film samples of various thicknesses. These data were taken at room temperature.

Cost

Current bulk thermoelectric power modules are predicted to cost somewhat less than \$1/Watt when produced in high volumes. Similar quantum well modules are predicted to cost less than \$0.20/Watt in large volume production. The cost of cooling modules will be somewhat less on a per watt basis. The reason

for the predicted lower cost of quantum well devices is due both to their higher efficiency and the fact that they are made from lower cost raw materials than bulk thermoelectrics.

Hi-Z's current quantum well film production rate is quite low because of the size of our laboratory machine. Our current quantum well programs will allow us to obtain a much larger machine in the very near future. In addition, we are working with Pacific Northwest National Laboratories (PNNL) under the sponsorship of Department of Energy (DOE) to investigate production scale up of quantum well films. In addition, Hi-Z is also investigating alternative means, such as CVD, to fabricate quantum well films at higher rates.

Assuming linear behavior, at a 2°C ΔT
efficiency will be $10\% \cdot \frac{2}{50} = 0.4\%$

$\bar{v} = 0.2\% / ^\circ\text{C}$

Discussion

Hi-Z has recently measured power and efficiency demonstrating a QW couple conversion efficiency of 14%. These measurements were made recently on a small couple that combined a multilayer QW of P type B_xC/B_yC with a QW of N type Si/SiGe. This couple operated between 70°C and 250°C and was fabricated on a 5 μm thick Si substrate with ~11 μm QW film thickness. The 14% efficiency was calculated by dividing the power out of the couple by the power in. The 14% efficiency was obtained with no correction for any extraneous heat losses, such as through the Si substrate and the heater wires. The experimental set up also confirmed a known efficiency of ~5.5% for Bi₂Te₃ bulk alloys, assuring the data accuracy. The experimental data point and the predicted values agree quite well. A confirmation that these QW materials exhibit a much higher figure of merit than bulk alloys is that the maximum efficiency was achieved at a ratio of load resistance to QW couple resistance of ~2.6 yielding a ZT of 4.1 at T=250°C, shown in Figure 7. The Bi₂Te₃ bulk alloys meet their maximum efficiency at a resistance ratio of ~1.2 when their ZT value is close to 1.

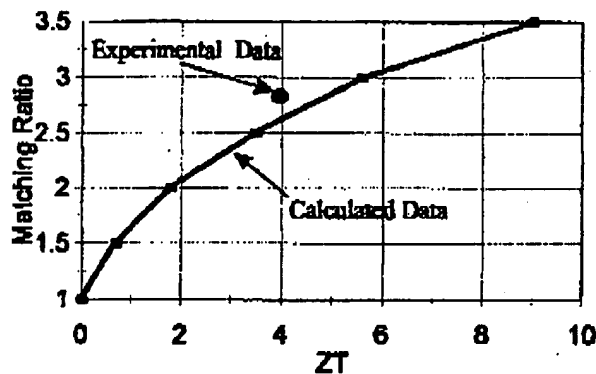


Figure 7: Matching ratio versus ZT for 11 μm thick QW film on 5 μm thick Si substrate.

In another separate experiment, the B_xC/B_yC film was used as a cooler creating a maximum temperature difference of ~45°C. This temperature difference gives ZT~3 for T~25°C. For this experiment, the P-type B_xC/B_yC was joined to small Cu wire. The QW film was the same material and thickness as used in the couple iteration above for the power generation systems, without the use of gases or moving parts.

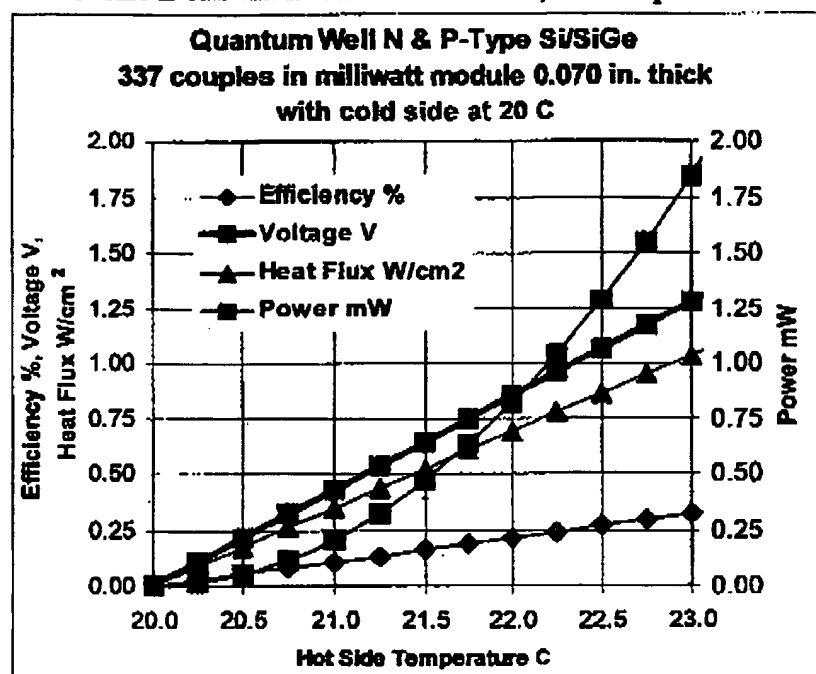
Acknowledgments

We would like to thank Mr. John Fairbanks of the Office of Heavy Duty Transportation in the Department of Energy for his support for this work.

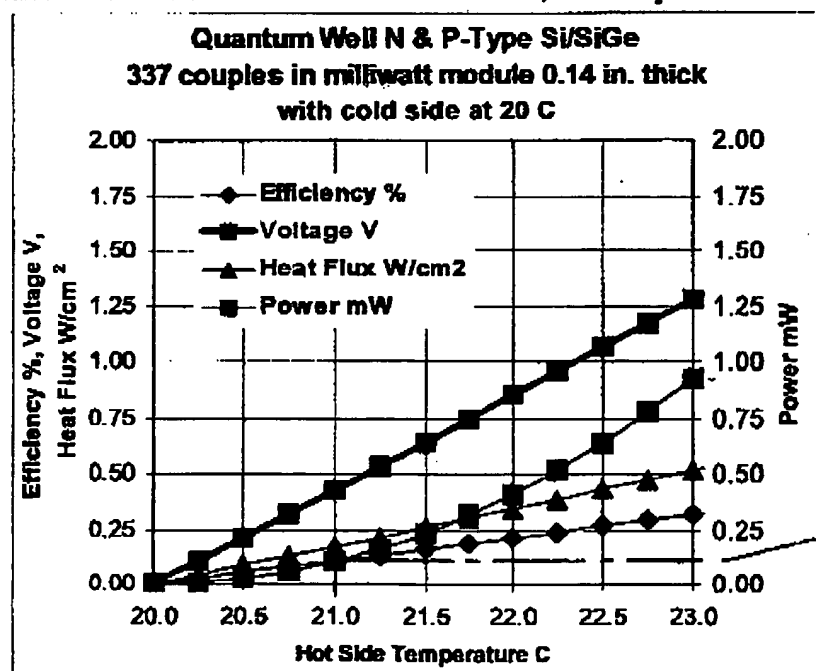
References

1. Harman, T.C., "PbTeSe/BiSb Short Period Superlattices as a New Thermoelectric Cooling Material," *Proc. 1st Natl. Thermogenic Cooler Conf.*, Center for Night Vision and Electro-Optics, U.S. Army, Ft. Belvoir, VA, 1992
2. S. Ghannaty, N. Elsner, K. Wang and Q. Xiang, "Thermoelectric Performance of B_xC/B_yC Heterostructures", ICF 1996, Pasadena, California.
3. Hicks, L.D., Dresselhaus, M.S., "Effect of Quantum-Well Structures on the Thermoelectric figure of Merit," *Phys. Rev. B*, 47, 19 (1993) 12 727-731.
4. "Proof-of-Principle Test for the thermoelectric Generator for Diesel Engines", 1991, Final Report, Hi-Z Technology, Inc., HZ 72691-1.
5. Elsner, N.B., Ghannaty, S., Norman, J.H., Farmer, J.C., Foreman, R.J., Summers, L.J., Olsen, M.L., Thompson, P.R. and Wang, K., 1994, "Thermoelectric Performance of $Si_{0.8}Ge_{0.2}/Si$ Heterostructures by MBE and Sputtering", Proceedings, 13th International Conference on Thermoelectrics, AIP Press, Kansas City, MO.
6. Ghannaty, S., 2002, "Quantum Well Thermoelectric Devices", Proceedings, DARPA/ONR/DOE High Efficiency Thermoelectric Workshop, Coronado, CA.

Quantum well milliwatt module with 676 elements 0.010 in. x 0.010 in x 0.07 in thick; eight 11 micron quantum well films on 25 micron Kapton in each element; module size is 0.29 in. x 0.29 in. x 0.070 in.; 337 couples.



Quantum well milliwatt module with 676 elements 0.010 in. x 0.010 in x 0.140 in thick; eight 11 micron quantum well films on 25 micron Kapton in each element; module size is 0.29 in. x 0.29 in. x 0.140 in.; 337 couples.



Quantum Well Milliwatt Module 0.29 in square

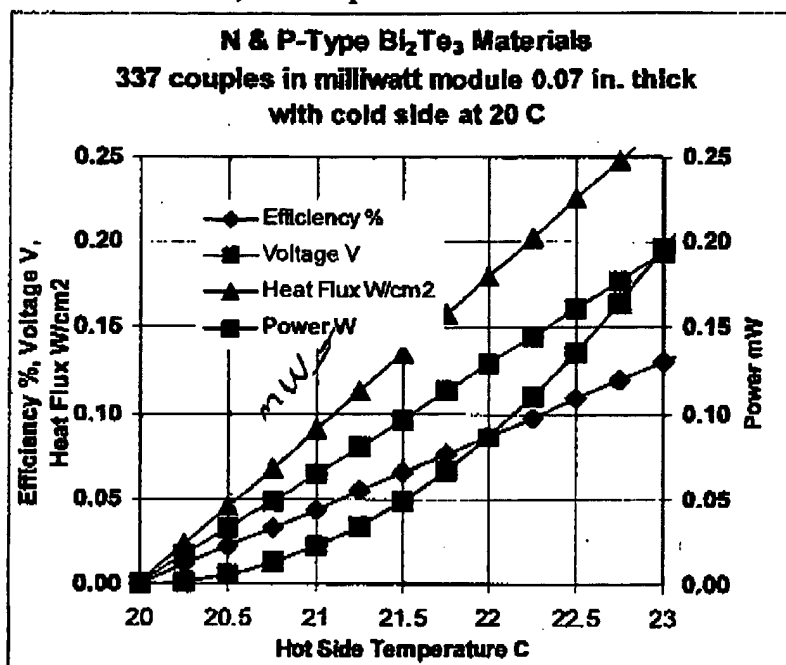
(2) x 676 elements = 170 in² resulting in 0.347% fill of 100 mW @ 1°C
 Each device yields $\frac{100}{(-3)} \approx 11 \mu\text{W}$ ($\times 2 = 22 \mu\text{W}$)

Results Summary

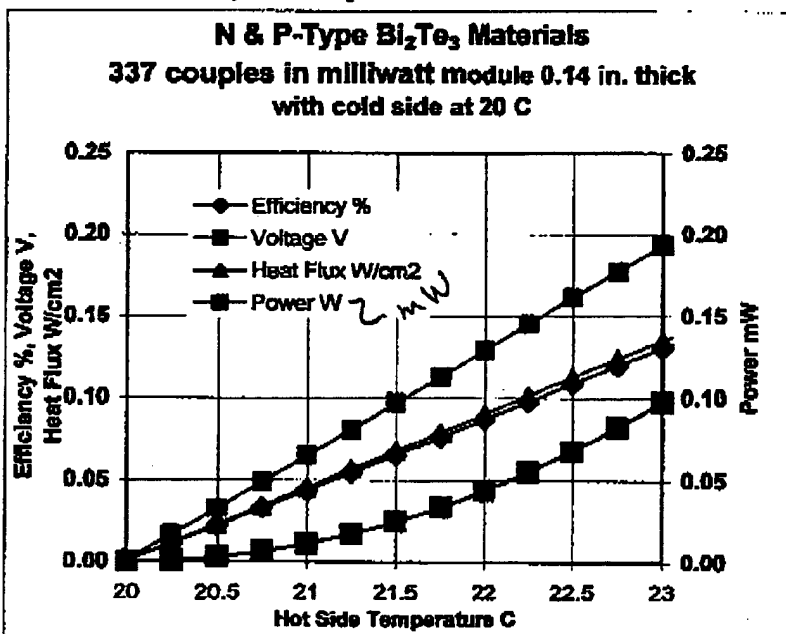
- TIE Device dimensions are 20 mm by 20 mm
- TIE Device thermal conductivity = $1.64 \times$ Fill Factor (W/mK)

Fill Factor	ΔT ($^{\circ}$ C)	ΔT ($^{\circ}$ C)	ΔT ($^{\circ}$ C)
	1 mm	2 mm	4 mm
25 %	0.073	0.136	0.249
50 %	0.040	0.075	0.143
75 %	0.029	0.053	0.102
100 %	0.023	0.042	0.079

Bismuth telluride alloy milliwatt module with 676 elements 0.010 in. x 0.010 in x 0.070 in thick; elements separated by 25 micron Kapton; module size is 0.29 in. x 0.29 in. x 0.070 in.; 337 couples.



Bismuth telluride alloy milliwatt module with 676 elements 0.010 in. x 0.010 in x 0.140 in thick; elements separated by 25 micron Kapton; module size is 0.29 in. x 0.29 in. x 0.140 in.; 337 couples.



Quantum Well Milliwatt Module 0.29insquare

**This Page is Inserted by IFW Indexing and Scanning
Operations and is not part of the Official Record**

BEST AVAILABLE IMAGES

Defective images within this document are accurate representations of the original documents submitted by the applicant.

Defects in the images include but are not limited to the items checked:

- BLACK BORDERS**
- IMAGE CUT OFF AT TOP, BOTTOM OR SIDES**
- FADED TEXT OR DRAWING**
- BLURRED OR ILLEGIBLE TEXT OR DRAWING**
- SKEWED/SLANTED IMAGES**
- COLOR OR BLACK AND WHITE PHOTOGRAPHS**
- GRAY SCALE DOCUMENTS**
- LINES OR MARKS ON ORIGINAL DOCUMENT**
- REFERENCE(S) OR EXHIBIT(S) SUBMITTED ARE POOR QUALITY**
- OTHER:** _____

IMAGES ARE BEST AVAILABLE COPY.

As rescanning these documents will not correct the image problems checked, please do not report these problems to the IFW Image Problem Mailbox.